# DYNAMIC CHARACTERISATION OF PASSIVE PORCINE SKELETAL MUSCLE USING IMPACT HAMMER: INLINE RESPONSES

Ya Huang[1]
[1]School of Engineering
University of Portsmouth
Portsmouth, PO1 3DJ
UK

Michael Takaza[2], Ciaran Simms[2]
[2]Department of Mechanical and Manufacturing Engineering
Trinity College Dublin
Dublin 2
Ireland

**Abstract**

Impulse responses of freshly harvested skeletal muscle specimens are presented for the first time using an impact hammer. The mass-tissue assembly represents a single degree of freedom mass-spring-damper system with the mass end free to move. The specimens were extracted from one thigh of a freshly sacrificed pig of approximately three-month old. The sprung mass was 2.5 kg with a flat and a hip-borne indentation interface with the tissue. With the impact force exerted in the vertical z-axis of the mass, the accelerance exhibited resonances at around 25 Hz and 40 Hz. With horizontal x-axis impacts, a single resonance appeared at around 2 to 3 Hz with its peak magnitude almost half of the peak magnitude obtained from the vertical impact. The magnitude of impact and thickness of specimen seemed to have little effect on the resonance frequencies. The specimen thickness from 10 to 20 mm has no clear effect on the parameters extracted.

## 1. Introduction

Force and motion transmitted to and through the human body during vibration, i.e. biodynamic responses, play a vital role in assessing health risks and evaluating of vibration isolation equipment. Key to the understanding of any biodynamic responses during whole-body vibration (WBV) is the dynamic behaviour of soft tissues at the excitation-subject interface, be it the buttocks of a seated, back of a recumbent or soles of a standing subject (Huang and Griffin, 2009). Skeletal muscle tissue deformation was found more than 50% larger than its adjacent fat tissue deformation (Shabshin et al., 2010). It is plausible that the skeletal muscle tissue at the interface plays a dominant role in the motion transmission path. Human vibration models calibrated by frequency response functions (FRFs), such as apparent mass and transmissibility, during base-excited vibration offer limited physical interpretation of the dynamic property of the interface soft tissue. Using frequency domain lumped parameter models, the principle dynamic stiffness (and damping constant) of a seated subject was 49 kN/m (615 Ns/m) at 0.25 $ms^{-2}$ r.m.s. of vertical random WBV, and 32 kN/m (522 Ns/m) at 2.0 $ms^{-2}$ r.m.s. (Huang and Griffin, 2006). With recumbent subjects, the same approach offered a stiffness of 60 kN/m (341 Ns/m) at 0.25 $ms^{-2}$ r.m.s. and 52 kN/m (433 Ns/m) at 1.0 $ms^{-2}$ r.m.s. (Huang and Griffin, 2008a). With longitudinal horizontal excitation, the stiffness was 16 kN/m (260 Ns/m) at the lower and 8.6 kN/m (217 Ns/m) at the higher magnitude (Huang and Griffin, 2008b). These values were seldom observed in meso-level biomechanics investigations of skeletal muscles.

Presented at the 50th United Kingdom Conference on Human Responses to Vibration, held at ISVR, University of Southampton, Southampton, England, 9 - 10 September 2015.

Existing biomechanics studies of porcine skeletal muscle tissue examined viscoelastic properties under cyclic and drop impact compressions in loading rates relevant to the car crashworthiness industry (Van Loocke et al., 2009; Takaza et al., 2013). The constitutive equations of tissues obtained from these studies were usually fed to numerical models of the human soft tissue so as to assess damage at higher frequencies and magnitudes of loading than those seen in human vibration. These formulations were not directly ready to offer analytical solutions and prediction of global responses.

During whole-body vibration, be it for a seated, standing or recumbent person, the principal resonance can usually be described by a single degree of freedom (SDOF) mass-spring-damper system. The loading and boundary condition of such model need to have a base excitation with the sprung mass end free to move (see Figure 1b). The majority of biomechanics studies investigating skeletal muscle tissue had both ends of the specimen clamped or compressed without any sprung mass. Similarly, hand-arm vibration studies required human subject to apply and maintain a push or grip force.


(a) SDOF with rigid foundation – impact hammer or shaker test

(b) SDOF with base motion – shaker test

Figure 1 Single degree of freedom (SDOF) mass-spring-damper system with rigid foundation (a) and base motion (b): *m*, *k*, and *c* are the sprung mass (in kg), dynamic stiffness (in N/m) and damping constant (in Ns/m) respectively; *f* ( *t* ) is the time history of input or excitation force (in N) provided by either a shaker or an impact hammer; $\ddot{z}(t)$ and $\ddot{z}_0(t)$ are the time histories of the resultant acceleration and excitation acceleration (in m/s$^2$).

One particular study looked into the dynamic characteristics of porcine skeletal muscle subjected to base excitation loaded with a sprung mass as an analogue SDOF (Aimedieu et al., 2003). With measured transmissibility between the base excitation and the resultant motion of the sprung mass, authors extracted frequency dependent dynamic stiffness and damping parameters so as to facilitate a finite element analysis of buttocks model for whole-body vibration in automotive seating applications. The stiffness and damping increased with increasing excitation frequency from 20 to 30 Hz. Damping was low from 5 to 20 Hz and increased to 556 Ns/m at 30 Hz. Mean stiffness ranged from 8.5 kN/m at 5 Hz to 347 kN/m at 30 Hz. The specimens were tested after 24 hours of animal death, storing at 4$^o$C and testing at 37$^o$C in a bath, while many other biomechanics tests were performed within 2 hours of animal death to minimise effects of rigor mortis (Takaza et al., 2013).

Impact hammer test, or so-called experimental modal test, has been a standardised procedure to extract frequency response functions of mechanical structures that are prone to dynamic stress and strain (Ewins, 2000). It offers a quicker and simpler setup comparing to a base-excited shaker test. However, the impact hammer modal test could only produce a frequency response function with a rigid foundation. If the dynamic material providing the coupling force were ideally homogeneous, linear and

isotropic, the estimated parameters m, k, and c would be the same in the two experimental setups seen in Figure 1. But the number of uncertainties involved in setting up soft tissue would mean that none of the above assumption could be honoured and the actual system measured comprises a multitude of nonlinear effects. Besides, different integral errors inherited in the two techniques also contribute to the estimations. The present study is intended to apply the impact hammer approach to a SDOF mass-tissue system in the context of whole-body vibration.

Many natural and artificial materials can be dynamically characterised by their viscoelastic properties – depicting the stiffness (-elastic) and damping (visco-) parameters. By formulating the equations of motion using the elastic modulus and loss factor, one can readily estimate the frequency dependent stiffness and damping parameters from an impact hammer test (Jones, 2001). The combination of base-excited transmissibility and lumped parameter models (e.g. Figure 1b) could only provide a linear estimation of the dynamic characteristics – a stiffness value and a damping value, as in a SDOF, constant for the whole range of frequency in question. While this is rarely true for most real systems, it is plausible to first compare the values of the stiffness and damping at the principle resonance frequencies so as to understand the variation in the impact hammer technique. The mathematical treatment of a SDOF linear viscoelastic material model is presented in Appendix A as part of the procedure in the method section of this study.

The present study intends to compare dynamic characteristics extracted from a impact hammer test of an analogue SDOF mass-tissue system in vitro to the parameters obtained from WBV calibrated lumped parameters (i.e. Huang and Griffin, 2006, 2008) and those measured with a base-excited in vitro setup (i.e. Aimedieu et al., 2003). From the existing literature and experimental experience, the extracted dynamic stiffness and damping are unlikely to be close to those observed during WBV, and tend to vary between different specimens (inter-specimen) and between different repeats using the same specimen (intra-specimen). One of the uncertainties of such in vitro setup would be response in the axes other than the axis of excitation – cross-axis response. Due to length, this paper will limit its discussion on the inline responses when the impact hammer exerts impact force in the vertical and horizontal axes respectively. The impact hammer approach is expected to be less time consuming comparing with a base-excited shaker test, giving the vital chance for experimenters to prepare and sample as many fresh specimens as possible in the time window of 2 hours after animal death.

**2. Method**

The experimental study is consisted of preparing and conducting impact hammer test on the sprung mass-muscle tissue analogue SDOF system, and signal processing of the time histories of excitation impact force and resultant acceleration measured at the sprung mass. The time domain data was then transformed into the frequency domain in the form of FRFs, first accelerance and then receptance. Using linear viscoelastic theories, the complex dynamic stiffness and damping were derived from the receptance function with the process depicted in Appendix A.

2.1 Apparatus

The sprung mass-skeletal muscle SDOF system was laid on a horizontally flat test bench that is rigidly attached to the ground (see Figure 2). The flat 2.5 kg sprung mass was made by rigidly compressing and bolting enough layers of lead discs onto a rigid smooth flat perplex plate, which in turn was in contact with the muscle tissue specimen beneath (Figure 2 b3a). The sprung mass and nominal footprint of the specimen (50 x 50 mm) was selected to represent a pressure approximately 10 kPa of a stationary sitting person. A second sprung mass of the same mass but with four evenly spaced semi-sphere protrusions, each with a diameter of 15 mm and evenly was distributed on a circle of 40 mm diameter to the centre of the base plate, was used to examine effects of indentation to the muscle specimen beneath while measuring the dynamic responses (Figure 2 b3b). The simple indenter shape was designed to imitate some feature of the bony structure of the ischial tuberosities in a seated subject. Therefore it is refer to as the 'hip-borne' sprung mass.

One channel of force from the force sensor on the Dytran 5800B4 impact hammer (sensitivity of 2.2 mV/N), and three channels of single-axis B&K4507 B006 (±14g) accelerometers arranged in 3 orthogonal axes and rigidly mounted on top of the sprung mass, were connected to ABUCUS data acquisition module with a signal analyser software SignalCalc-Mobilyser, DataPhysics®. Two to four repeat measurements of hits were taken from each test specimen. The variations in the time histories and their subsequent FRFs could be caused by the experimenter producing different directions, magnitudes and timings of hits.

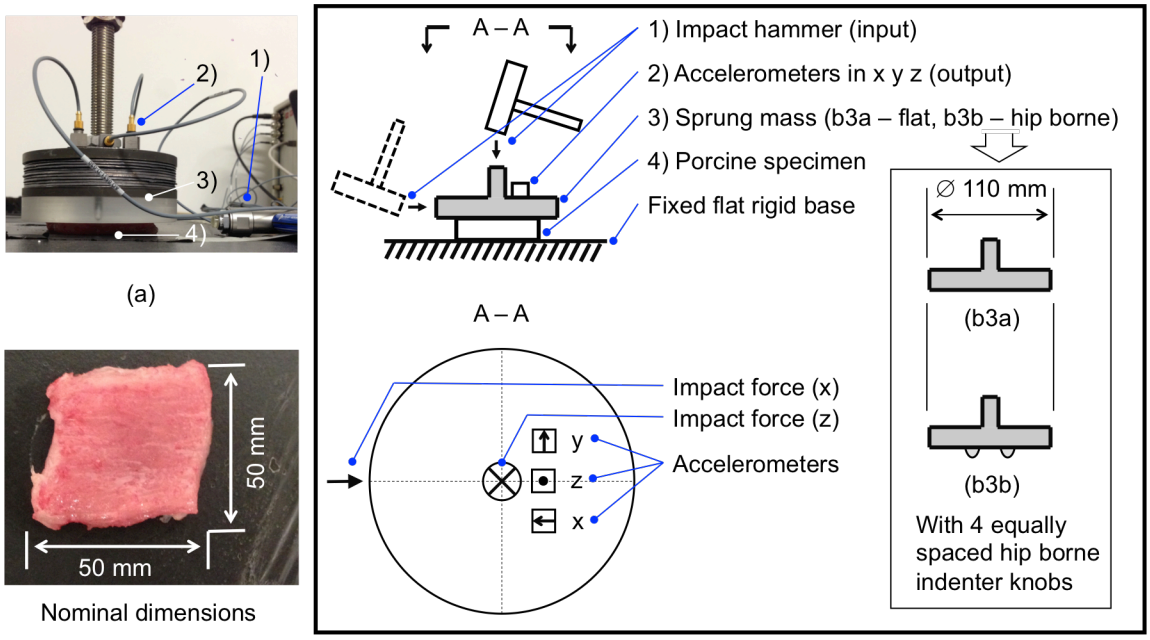


Figure 2 Photographic and schematic representations of the experimental setup: (a) and (b) the equipment and setup showing the impact hammer, the three accelerometers, the two types of sprung masses of 2.5 kg each; (c) the freshly obtained square porcine skeletal muscle specimen with a nominal dimension of 50 ±2 mm and three nominal thicknesses 10, 15 and 20 ±2 mm.

2.2 Stimuli

The ideal time history of the impact force would have a duration of zero, or as short as practically possible (see Figure 3 Excitation force), like a delta function in signal processing to give a flat frequency spectrum (see Figure 4 PSD – power spectral density functions – of the impact force). In the frequency domain, this is equivalent to a broadband random excitation but with limited sampling duration due to the short event. The frequency range of interest in the present study is up to 80 Hz. A hard rubber tip was used for the hammer to filter out unnecessary high frequency energy.

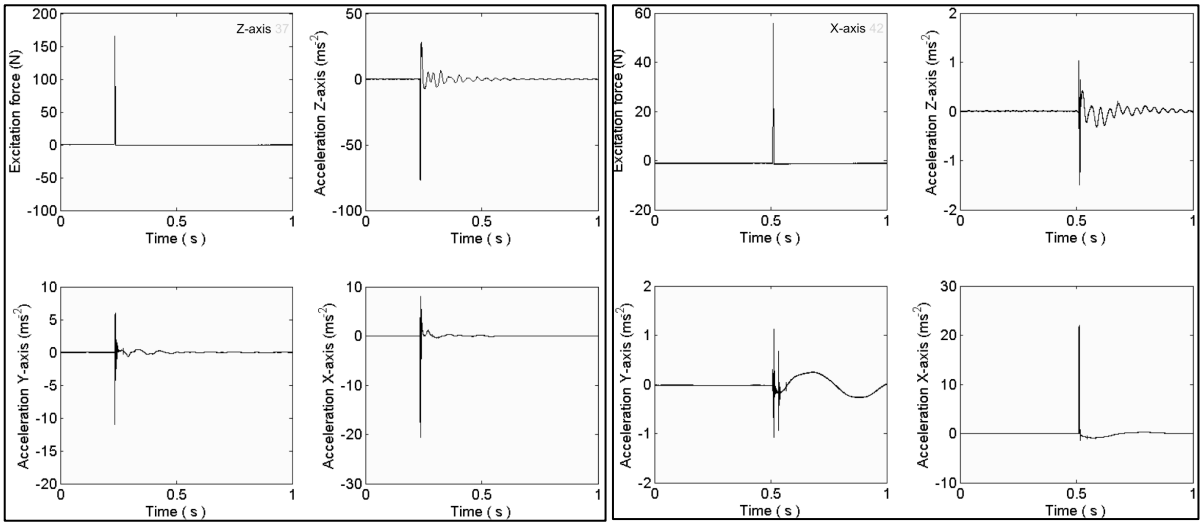


Figure 3 Example time histories of the impact excitation force and the three orthogonal axes of accelerations when the impact force was applied in the vertical z-axis (a) and horizontal x-axis (b) using a flat sprung mass and a 10 mm thick specimen (S7 in Table 1).

2.3 Specimen preparation

Skeletal muscle tissue samples were harvested from a 3 month old female pig. The experimental protocols were approved by the University of Dublin Ethics Committee. Porcine Gluteus Maximus muscle specimens were freshly harvested from one thigh in a nominal footprint of approximately 50 by 50 mm and thicknesses of 10, 15 and 20 mm (Figure 2). The specimens were cut using a scalpel so that the muscle fibres were roughly parallel to the plane of the flat test bench surface. So during the vertical z-axis impact, the compressive force was applied always in the cross-fibre direction; during the horizontal x-axis impact, the force could be applied either in the cross-fibre direction or in the fibre direction. The tests were conducted within two hours of animal death to minimise rigor mortis effects. The timeline of experimental procedure is partly depicted by Table 1.

2.4 Analysis

Based on the SDOF dynamic model in Figure 1a and an analytical formulation in Appendix A called 'omega arithmetic', one could utilise the measured complex FRF accelerance A(ω) = $\ddot{Z}(\omega)$ / F(ω), the ratio between resultant acceleration and input force in the angular frequency domain ω (rad/s), to calculate the complex receptance R(ω) = Z(ω) / F(ω), the ratio between resultant displacement and

input force. By applying linear viscoelastic formulations, it is possible to compute the frequency-dependent dynamic stiffness *k* (N/m) and damping *c* (Ns/m).

To capture each hit, the time histories of the impact force and three accelerations were acquired at 107520 samples per second for 1.219 second, i.e. a total of 131072 data points. By applying a fast Fourier transform (FFT) at this full length of data and a rectangular window, the PSDs and FRFs were computed at a frequency resolution of 0.8203 Hz.

**3. Results**

Nine specimens were tested within two hours of animal death (Table 1). With little statistical power, the limited number of specimens and tests still provided a sketch of the variation initially expected in the experimental plan. The results presented below intend to show: the inter-specimen and intra-specimen variation (Figure 4 and 5), effect of specimen thickness (Figure 6 and 7), and effect of the contact contours of the flat and hip-borne sprung masses (Figure 8). Guided by the timeline in Table 1, one could inspect the rigor mortis effect.

3.1 Inter-specimen and intra-specimen variation

With impact force exerted in the vertical axis of the sprung mass, the PSDs of the inline z-axis acceleration (Figure 4) and accelerance exhibited a principle resonance at around 25 Hz and a secondary at about 40 Hz. With horizontal x-axis impacts, the PSDs of the inline x-axis acceleration (Figure 5) and inline accelerance showed a single resonance around 3 Hz with its peak magnitude almost half of the peak magnitude obtained from the vertical impact. With each specimen subjected to several repeat hits, the resultant acceleration at peak (non-flat lines of the PSDs in Figure 4 and 5) increases with increasing impact force magnitude (flat lines of the PSDs in Figure 4 and 5). The frequencies at which the peak resultant acceleration occurred seemed to be the same for different repeats of the same specimen and the same for different specimens with or without the same thickness despite the experiment timeline.

3.2 Effect of specimen thickness

The frequency dependent stiffness *k* and damping *c* of the first three specimens (s1, s2, s3) each with different thicknesses showed a similar order of values for at the frequency of the first peak around 25 Hz for the vertical (Figure 6) and around 2.5 Hz for the horizontal impact (Figure 7). For vertical impacts, both stiffness and damping tended to increase with frequency in the range 20 to 30 Hz where the first peak of accelerance occurred; for horizontal impacts, the stiffness gradually increased and the damping slightly decreased as the frequency increased from 1 to 5 Hz where the first peak occurred.

Presenting the *k* and *c* values of the first peaks in Table 1 to Figure 8, it becomes clear that across the ten specimens tested with the flat sprung mass (s1 to s10), the stiffness *k* does not seem to vary consistently as the thickness increases from 10 to 15 and 20 mm with both vertical and horizontal impacts. But there is a slight reduction in damping as the thickness increases for vertical impacts.

Table 1 Extracted dynamic stiffness (k) and damping (c) parameters at the first principal peak frequency of accelerance when the specimens were subjected to vertical z-axis and horizontal x-axis impacts. Specimens S1 to S10 were pre-loaded with the flat 2.5 kg sprung mass, and S10hp and S3hp were the same specimens as S10 and S3 but pre-loaded with the hip-borne 2.5 kg sprung mass. Each specimen number comprised of 2 to 4 repeat runs using the impact hammer, and the k and c values were the averages from the repeats with their variability shown in the Figures as examples.

| Time after death (min) | Specimen number | Thickness (mm) | Vertical z-axis impact | | Horizontal x-axis impact | |
|---|---|---|---|---|---|---|
| | | | First peak (Hz) | k (kN/m)<br>c (Ns/m) | First peak (Hz) | k (kN/m)<br>c (Ns/m) |
| 48 | S1 | 10 | 25 | 53.6<br>136 | 2.5 | 0.497<br>15.0 |
| 60 | S2 | 15 | 25 | 65.3<br>89.5 | 3.3 | 0.810<br>10.3 |
| 68 | S3 | 20 | 25 | 68.1<br>77.8 | 2.5 | 0.889<br>13.6 |
| 76 | S4 | 10 | 25 | 65.1<br>84.3 | 3.3 | 0.497<br>11.5 |
| 85 | S7 | 10 | 25 | 65.1<br>100 | 3.3 | 0.522<br>18.0 |
| 92 | S5 | 15 | 25 | 58.9<br>75.0 | 2.5 | 0.373<br>9.73 |
| 97 | S8 | 15 | 25 | 54.5<br>118 | ——— | ——— |
| 112 | S6 | 20 | 24 | 51.4<br>89.6 | ——— | ——— |
| 118 | S9 | 20 | 25 | 65.9<br>85.4 | ——— | ——— |
| 153 | S10 | 10 | 25 | 51.2<br>87.6 | 1.6 | 0.267<br>10.5 |
| 158 | S10hp | 10 | 24 | 57.9<br>57.8 | 2.5 | 0.548<br>12.9 |
| 167 | S3hp | 20 | 23 | 54.4<br>54.6 | 2.5 | 0.473<br>8.74 |
| 172 | S11hp | 10 | 25 | 73.5<br>88.7 | 3.3 | 1.03<br>18.6 |

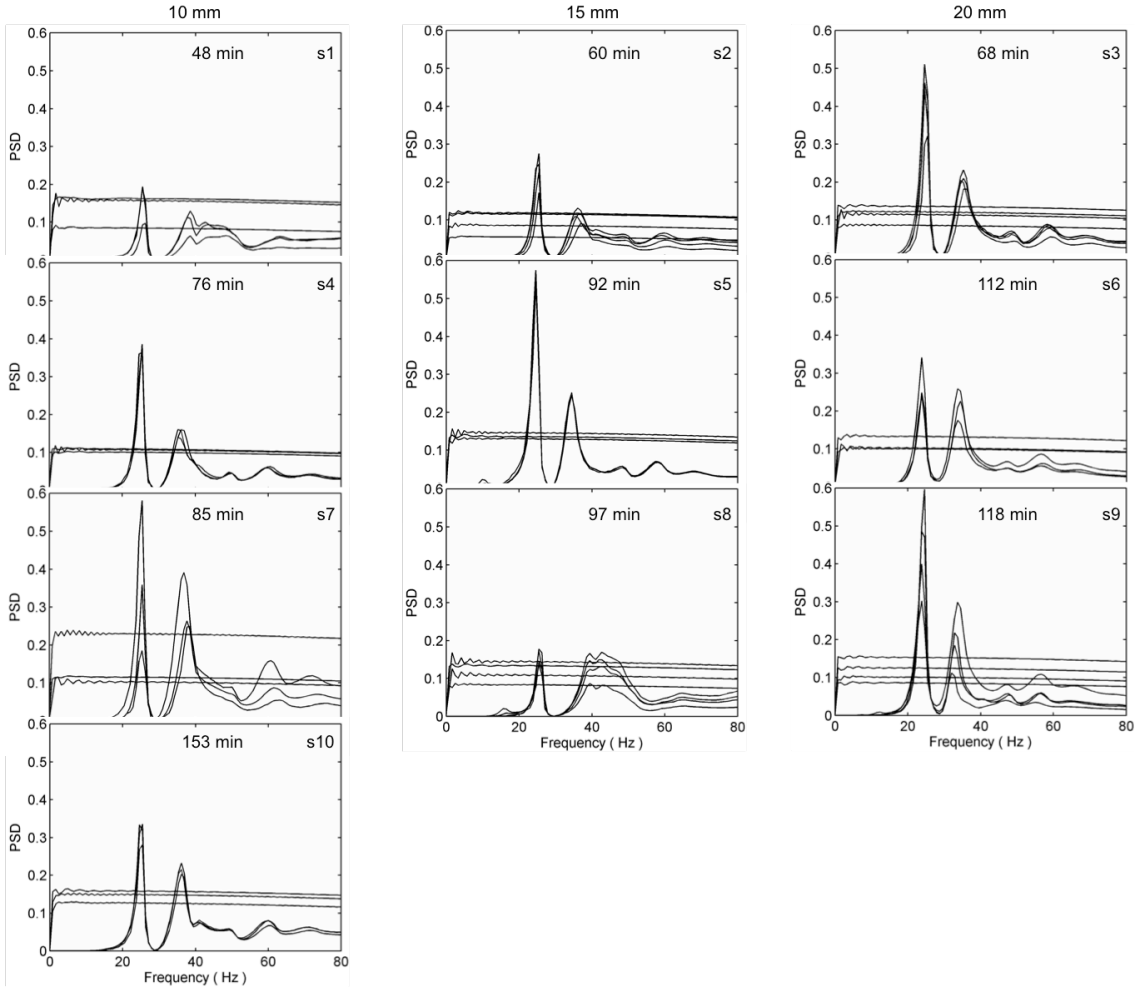


Figure 4 Vertical z-axis impact with flat sprung mass: PSDs of impact force (flat lines, $N^2$/Hz) and resultant acceleration (non-flat lines, $(m/s^2)^2$/Hz) of 10 specimens (s1 to s10 each with several repeat runs) showing time of test from animal death.

3.3 Effect of sprung mass contact contour

Specimen and test s10, and test s10hp, are selected to show the effect of the hip-borne sprung mass. For vertical impacts, the accelerance and receptance with the hip-borne sprung mass show distinctive higher magnitude and lower frequency of the first peak than those of the flat sprung mass in the frequency range 20 to 30 Hz (Figure 9a). This trend is less clear in the horizontal case but still appreciable in the narrower frequency range of 1 to 5 Hz (Figure 9b). Comparing solid markers in Figure 8 (and Table 1) extracted from *k* and *c* of Figure 9 with the hollow markers, the stiffening effect of the hip-borne sprung mass is the most obvious with the thinnest specimen (10 mm) in both vertical and horizontal impacts. There tends to be a reduction in damping by using the hip-borne sprung mass during vertical impact, but no apparent effect for horizontal impacts (Figure 8).

**4. Discussion**

With cross-fibre vertical impacts, the PSDs of different specimens consistently show two main resonances at around 25 and 40 Hz. This bimodal response contrasts with the single resonance

observed in apparent mass of vertical WBV – 4 to 6 Hz for seated (Huang and Griffin, 2006), and 8 to 10 Hz for recumbent (Huang and Griffin, 2008a). The more varied PSDs at above 40 Hz may be due to variation in the microstructure of muscle tissues, i.e. fibre, fascicles, and connective tissues. Different specimens could have different geometric characteristics of the microstructure. Fluid expulsion could be a contributor to the difference between the in vivo configuration in a human subject and the in vitro setup in the present study. The highest velocity of the sprung mass, compressing the muscle tissue, after impact was less than 0.2 m/s comparing to the drop impact velocity of up to 3 m/s in the study conducted by Takaza et al. (2013), who reported an average of 8% fluid mass loss.

With horizontal impacts, the PSDs of different specimens repeatedly show a main resonance at around 2 to 3 Hz. The frequency is similar to that observed in apparent mass of recumbent human subjects during horizontal longitudinal WBV (Huang and Griffin, 2008b). It is plausible that when the passive muscles are subjected to shear (horizontal) load, the present in vitro setup shares a similar motion transmission mechanism to the back of a recumbent human. While with (vertical) compressive loading the test differs to the human response with a largely non-homogeneous sprung mass.

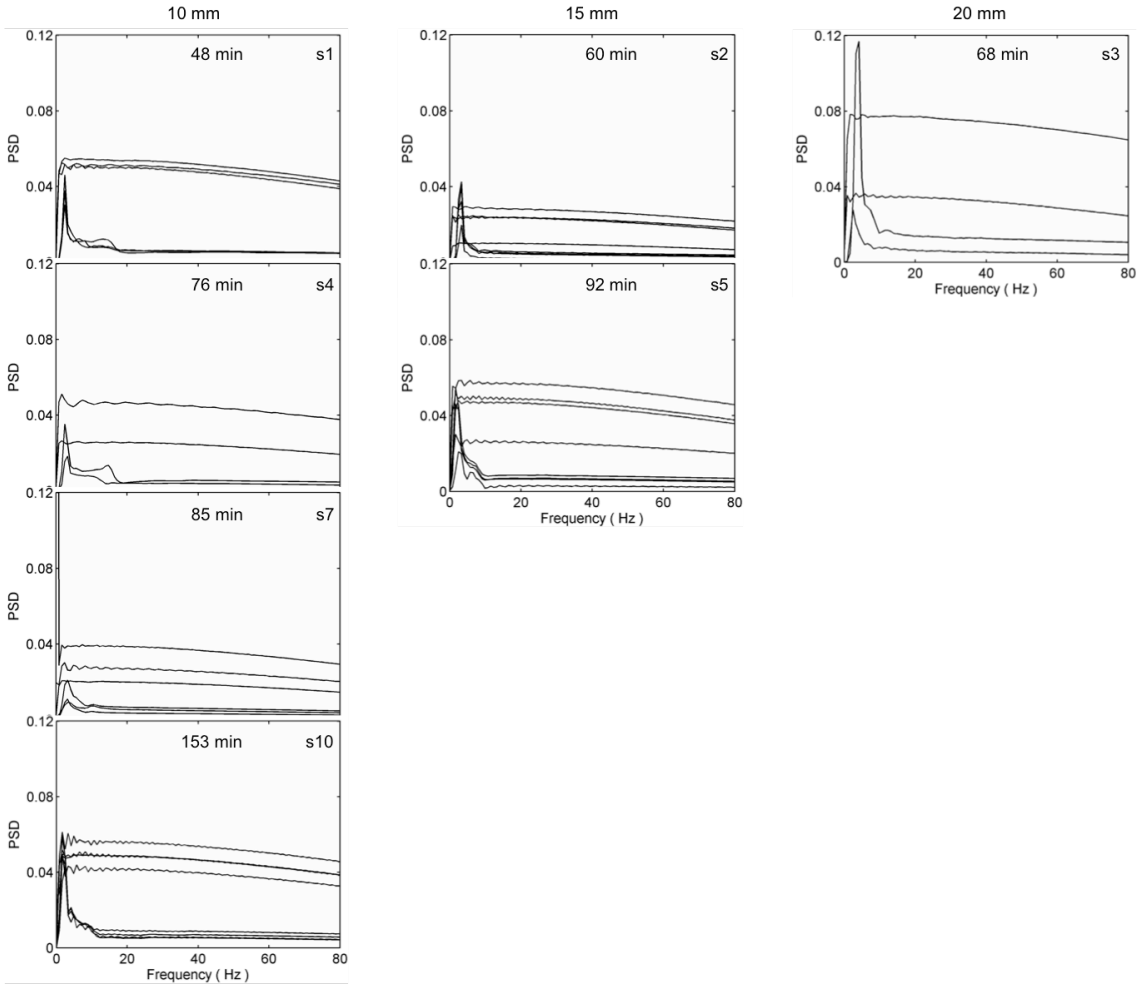


Figure 5 Horizontal x-axis impact with flat sprung mass: PSDs of impact force (flat lines, $N^2$/Hz) and resultant acceleration (non-flat lines, $(m/s^2)^2$/Hz) of 7 of the 10 specimens (s1 to s10 each with several repeat runs) showing time of test from animal death.

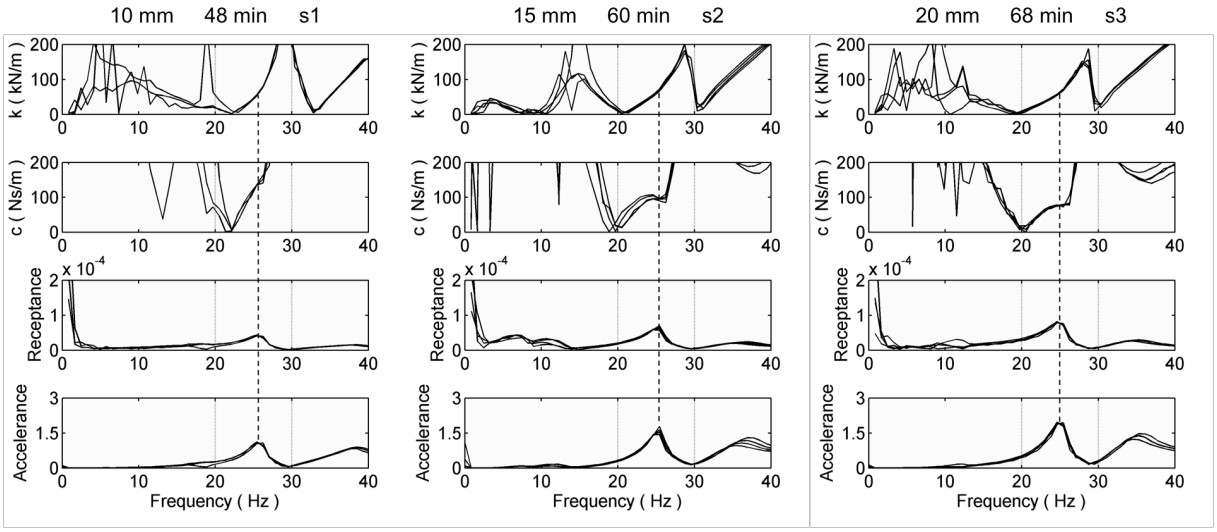


Figure 6 Vertical z-axis impact with 2.5 kg flat sprung mass: column 1 for s1 with thickness and time after death, column 2 for s2, and column 3 for s3. For each specimen (s1 to s3) the dynamic stiffness k, damping c, receptance ($s^2$/kg), and accelerance (1/kg) are shown. Frequency of interest: 20 to 30 Hz, with vertical dashed line indicating the peak around 25 Hz. Refer to Table 1 for values.

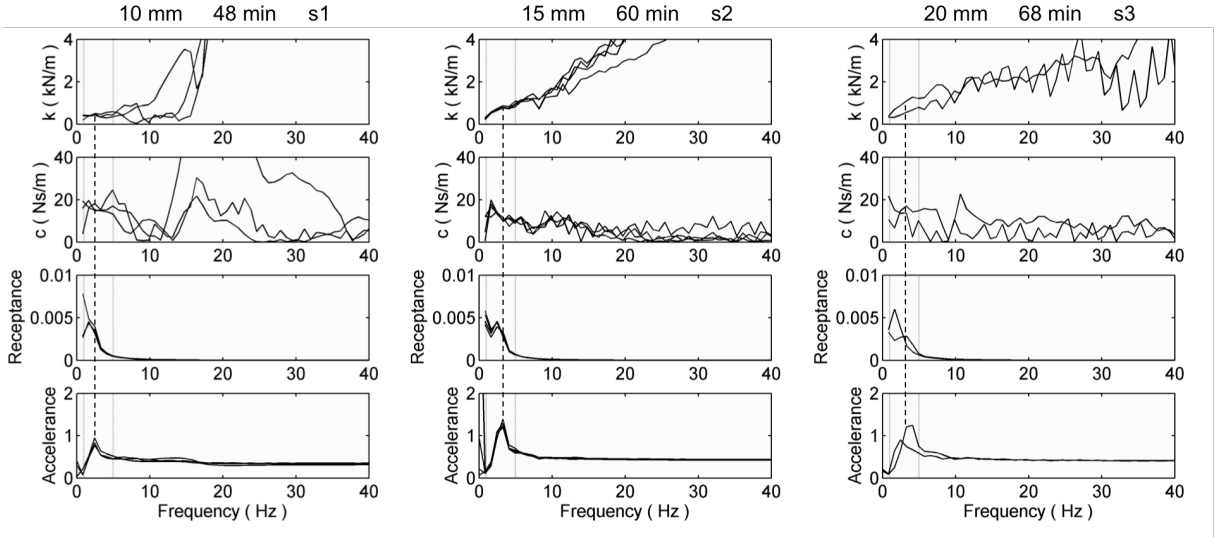


Figure 7 Horizontal x-axis impact with 2.5 kg flat sprung mass: column 1 for s1 with thickness and time after death, column 2 for s2, and column 3 for s3. For each specimen (s1 to s3) the dynamic stiffness k, damping c, receptance ($s^2$/kg), and accelerance (1/kg) are shown. Frequency of interest: 1 to 5 Hz, with vertical dashed line indicating the peak around 2.5 Hz. Refer to Table 1 for values.

The stiffness values obtained from lumped parameter models of seated (Huang and Griffin, 2006) and recumbent (Huang and Griffin, 2008a) subjects during vertical base-excited WBV presented in Figure 8 as horizontal solid and dashed lines. They show similar order to the current study. The damping for vertical excitation and both stiffness and damping for horizontal excitation of recumbent subjects

(Huang and Griffin 2008b) are far higher than those observed in the present study – see Introduction. This raises the question whether the FRFs, e.g. accelerance, or the linearly derived frequency-dependent stiffness and damping is a better quantification tool for dynamic characterisation. Accelerance is directly measurable, however, it lacks intuitive physical interpretation. Stiffness and damping offer straightforward comparison to other studies of different setups, but rely on the receptance that is computed from accelerance with inherited integral errors especially at lower frequencies, e.g. up to around 1 to 2 Hz – a range relevant to the horizontal WBV.

FRFs of whole-body vibration exhibit responses in axes orthogonal to the axis of excitation and are highly correlated to the inline response (Huang, 2012). This cross-axis response could offer explanation for the deviation in the dynamic parameters. Two uniformly contoured sprung masses were used in the present study to minimise inherit cross-axis response. But the difficulty in preparing uniform specimen caused by its soft nature and the variations in the muscle microstructure would inevitably result in cross-axis response for both vertical and horizontal impacts.

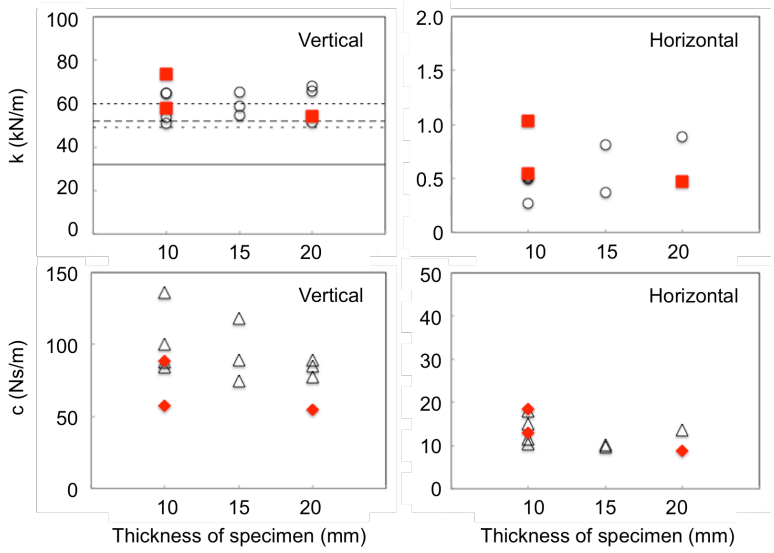


Figure 8 Dynamic stiffness (first row) and damping constant (second row) at the first peak frequency for vertical (left column) and horizontal (right column) using three thicknesses of specimens (10, 15 and 20 mm) with flat (hollow circle and triangle) and hip-borne sprung mass (solid square and diamond), values in Table 1. Stiffness from vertical WBV of seated (. . .) and recumbent (…) at 0.25 $ms^{-2}$ r.m.s.; seated (__) and recumbent (- - -) at 1.0 $ms^{-2}$ r.m.s. by Huang and Griffin (2006, 2008a).

**5. Conclusions**

Impulse responses of freshly harvested skeletal muscle specimens are presented for the first time. A linear SDOF viscoelastic model was utilised to extract stiffness and damping from the measured accelerance and receptance frequency response functions. A repeatable bimodal accelerance is observed for the (cross fibre) vertical impact tests at around 25 and 40 Hz – a higher frequency range than those observed in vertical WBV. Microstructure and the fluid-structure interaction of the muscle fibre and fascicle may be responsible for the responses at frequencies above 40 Hz. A repeatable peak accelerance is observed for the horizontal impact tests at around 3 Hz – similar to that observed in horizontal WBV. The specimen thickness has no clear effect on the parameters extracted.

(a) Vertical z-axis impact s10 (- -) and s10hp (**- -**)

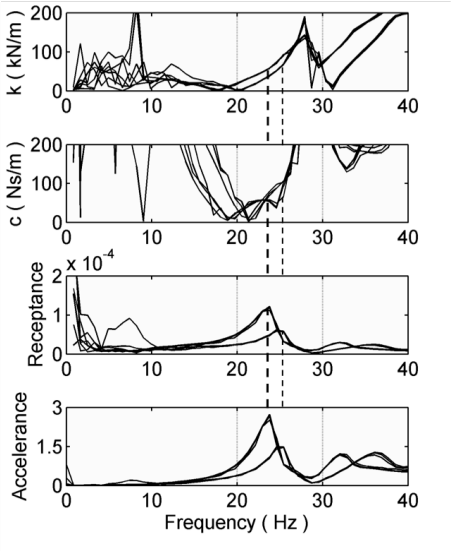


(b) Horizontal x-axis impact s10 and s10hp (**- -**)

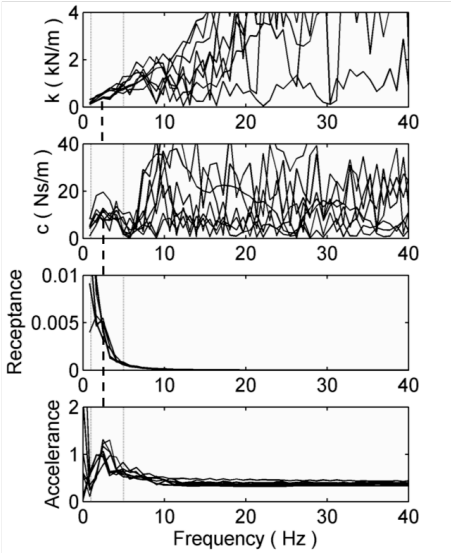


Figure 9 Specimen 10 tested approximately 153 minutes after death: Vertical z-axis impact (a) and horizontal x-axis impact (b) with 2.5 kg flat sprung mass (s10, vertical thin dashed line) and 2.5 kg hip-borne sprung mass (s10hp, vertical thick dashed line). Refer to Table 1 for values at peak.

## 6. References


Aimedieu, Jr P, Mitton, D, Faure, JP, Denninger, L, Lavaste, F (2003). Dynamic stiffness and damping of porcine muscle specimens. Medical Engineering and Physics, 25, pp795 – 799.

Ewins DJ (2000). Modal Testing: Theory, Practice & Application. Research Studies Press Ltd.

Huang Y (2012). Principal component analysis and virtual coherence of the cross-axis apparent mass in whole-body vibration. Proceedings of the 47th United Kingdom Conference on Human Responses to Vibration, Institute of Sound and Vibration Research, University of Southampton, Southampton, England, 17 – 19 September.

Huang, Y, Griffin, MJ (2006). Effect of voluntary periodic muscular activity on nonlinearity in the apparent mass of the seated human body during vertical random whole-body vibration. JS&V, 298.

Huang, Y, Griffin, MJ (2008a). Nonlinear dual-axis biodynamic response of the semi-supine human body during vertical whole-body vibration. Journal of Sound and Vibration, 312, pp296 – 315.

Huang, Y, Griffin, MJ (2008b). Nonlinear dual-axis biodynamic response of the semi-supine human body during longitudinal horizontal whole-body vibration. JS&V, 312, pp273 – 295.

Huang, Y, Griffin, MJ (2009). Nonlinearity in apparent mass and transmissibility of the supine human body during vertical whole-body vibration. JS&V, 324, pp429 – 452.

Jones, DIG (2001). Hand Book of Viscoelastic Vibration Damping. John Wiley & Sons Ltd. England.

Shabshin, N, Ougortsin, V, Zoizner, G, Gefen, A (2010). Evaluation of the effect of trunk tilt on compressive soft tissue deformations under the ischial tuberosities using weight-bearing MRI. Clinical Biomechanics, 25, pp402 – 408.

Takaza, M, Moerman, KM, Simms, CK (2013). Passive skeletal muscle response to impact loading: Experimental testing and inverse modelling. Journal of the Biomechanical Behavior of Biomedical Materials, 27, pp214 – 225.

Ungar, EE, Kerwin, EM (1962). Loss factors of viscoelastic systems in terms of energy concepts. The Journal of the Acoustical Society of America, 34 (7), pp954 – 957.

Van Loocke, M, Simms, CK, Lynos, CG (2009). Viscoelastic properties of passive skeletal muscle in compression – Cyclic behaviour. Journal of Biomechanics, 42, pp1038 – 1048.

## Appendix A Dynamic stiffness, damping, receptance and accelerance for the SDOF system

Equation of motion (EOM) of the SODF in Figure 1a:

$$m\ddot{z} + c\dot{z} + k z = f(t) \quad \text{(A1)}$$

Rearrange the above using complex dynamic stiffness k*:

$$m\ddot{z} + k^* z = f(t) \quad \text{(A2)}$$

where $k^* = k(1 + i\eta)$, and $\eta$ the loss factor: the energy dissipation per radian to the peak potential energy in a cycle.

According to similar formulations by Ungar and Kerwin (1962):

$$c = |k|\,\eta / \omega \quad \text{(A3)}$$

where ω is the angular frequency in rad/s, |k| is the modulus of the complex stiffness k in N/m. Then,

$$m\ddot{z}(t) + k(1+ i\eta)\, z(t) = f(t) \quad \text{(A4)}$$

Taking Fourier transform of the above:

$$m(-\omega^2)Z(\omega) + k(\omega)(1+ i\,\eta(\omega))\, Z(\omega) = F(\omega) \quad \text{(A5)}$$

Receptance as a complex frequency response function can be written as:

$$R(\omega) = \frac{Z(\omega)}{F(\omega)} = \frac{1}{k(\omega)[(1 - r^2) + i\,\eta(\omega)]} \quad \text{(A6)}$$

where $r = \frac{\omega}{\omega_n}$ is the frequency ratio, $\omega_n = \sqrt{k/m}$ is the natural frequency in rad/s, *F(ω)* and *Z(ω)* are the frequency domain equivalence of *f(t)* and *z(t)*.

The complex FRF, R(ω), is obtained from measured accelerance (e.g. by impact hammer) A(ω) = $\ddot{Z}(\omega)$ / F(ω) using 'Omega arithmetic':

$$R(\omega) = A(\omega) / (-\omega^2) \quad \text{(A7)}$$

The real and the imaginary parts of R(ω) can be used to find *k* and *η* from (A6):

$$Re(R) = \frac{1- r^2}{k[(1 - r^2)^2 + \eta^2]} \quad \text{(A8)}$$

$$Im(R) = \frac{-\eta}{k[(1 - r^2)^2 + \eta^2]} \quad \text{(A9)}$$

The frequency dependent *k* and *η* can then be estimated by:

$$k(\omega) = \frac{Re(R)}{|R|^2 (1- r^2)} = \frac{Re(R)}{|R|^2} + m\omega^2 \quad \text{(A10)}$$

$$\eta(\omega) = \frac{Im(R)}{Re(R)} (r^2 - 1) = \frac{Im(R)}{Re(R)} \left(\frac{m\omega^2}{k} - 1\right) \quad \text{(A11)}$$

Where |R| is the modulus of the measured complex receptance.

The frequency dependent damping constant *c*(ω) can finally be determined by (A3) above.